Journal of Building Engineering

Optimum Seismic Design of Frame Structures with and without Metallic Yielding Dampers Considering Life-Cycle Cost

--Manuscript Draft--

Manuscript Number:	JBE-D-23-03326
Article Type:	Research Paper
Section/Category:	Structural design
Keywords:	Seismic design; Life-cycle cost; FEMA P-58; Optimization; Yielding metallic device
Corresponding Author:	Abbas Karamodin Ferdowsi University of Mashhad Mashhad, Razavi Khorasan IRAN, ISLAMIC REPUBLIC OF
First Author:	Saeed Haji Rezazadeh Sanati, PhD Candidate
Order of Authors:	Saeed Haji Rezazadeh Sanati, PhD Candidate
	Abbas Karamodin
Abstract:	This paper investigates the optimal design of steel moment-resisting frame (MRF) buildings, with and without metallic yielding dampers, using a life-cycle cost (LCC)-based optimal design process. The aim is to minimize the LCC as the design criteria, including construction cost and loss of the lifetime seismic consequences. The study uses the endurance time (ET) method for structural response analysis and the comprehensive FEMA P-58 procedure for seismic loss assessment. Four design approaches, including typical code-based design of an existing MRF without damper, optimal LCC-based design of a new MRF without damper, optimal LCC-based design of an existing MRF equipped with damper, and optimal LCC-based design of a new MRF equipped with damper, are investigated. The results of the study highlight the effectiveness of the LCC-based optimal design process for achieving the desired balance between initial construction cost and seismic losses. Additionally, the study adds to the literature by examining the performance difference between an optimal designed frame without damper and an existing frame optimally equipped with damper, and the performance difference between an existing frame optimally equipped with damper and a new frame optimized simultaneously with damper. The results show that adding dampers to properly designed existing structures can sufficiently improve performance without the need to design a new building with damper.
Suggested Reviewers:	Farzin Zareian, PhD Professor, University of California Irvine zareian@uci.edu Expert in the field of earthquake engineering and performance-based design
	Iman Hajirasouliha, PhD Professor, The University of Sheffield i.hajirasouliha@sheffield.ac.uk Expert in the field of Life-cycle cost-based design and performance-based earthquake engineering.
	S. Ali Mirfarhadi, PhD Professor, Sharif University of Technology sa.mirfarhadi7@sharif.edu Expert in the field of Endurance Time method and Life-cycle cost-based optimization.
Opposed Reviewers:	

Cover Letter

Ferdowsi University of Mashhad
Department of Civil Engineering

April 22th, 2023

Dear Professor J. M. LaFave,

Enclosed please find a copy of a manuscript entitled "Optimum Seismic Design of Frame Structures with and without Metallic Yielding Dampers Considering Life-Cycle Cost" by S.H. Sanati and A. Karamodin that I am submitting to the *Journal of Building Engineering* for possible publication.

This paper investigates and compares different building design scenarios with and without dampers, using an LCC-based optimal design process. The study addresses the limitations of related literature by employing the ET method and the FEMA P-58 methodology for performance assessment within the optimization process. Additionally, the study adds to the literature by examining the performance difference between an optimal designed frame without damper and an existing frame optimally equipped with damper, and the performance difference between an existing frame optimally equipped with damper and a new frame optimized simultaneously with damper. The results show that adding dampers to properly designed existing structures can sufficiently improve performance without the need to design a new building with damper. The authors hope that this paper turns out to be interesting to the respected audience of the *Journal of Building Engineering*.

We confirm that this manuscript has not been published elsewhere and is not under consideration by another journal. All authors have approved the manuscript and agree with its submission to the *Journal of Building Engineering*.

Please do not hesitate to contact me if further information is required.

Your consideration is fully appreciated.

Best regards,

A. Karamodin (Ph.D.)
Associate Professor
Department of Civil Engineering,
Faculty of Engineering,
Ferdowsi University of Mashhad, Mashhad, Iran
E-mail: a-karam@um.ac.ir

Highlights:

- Developing an efficient LCC-based design procedure which employs ET analysis and FEMA P-58 methodology
- Instigating the performance difference between an optimal designed frame without damper and an existing frame optimally equipped with damper
- Instigating the performance difference between an existing frame optimally equipped with damper and a new frame optimized simultaneously with damper
- LCC-based design outcomes perform significantly better than the code-based outcomes
- Adding dampers to properly designed existing structures can sufficiently improve performance without the need to design a new building with damper

Optimum Seismic Design of Frame Structures with and without Metallic Yielding Dampers Considering Life-Cycle Cost

Saeed H. Sanati[*], Abbas Karamodin[1,*]

[*] Department of Civil Engineering, Faculty of Engineering, Ferdowsi University of Mashhad, Mashhad, Iran

Abstract

This paper investigates the optimal design of steel moment-resisting frame (MRF) buildings, with and without metallic yielding dampers, using a life-cycle cost (LCC)-based optimal design process. The aim is to minimize the LCC as the design criteria, including construction cost and loss of the lifetime seismic consequences. The study uses the endurance time (ET) method for structural response analysis and the comprehensive FEMA P-58 procedure for seismic loss assessment. Four design approaches, including typical code-based design of an existing MRF without damper, optimal LCC-based design of a new MRF without damper, optimal LCC-based design of an existing MRF equipped with damper, and optimal LCC-based design of a new MRF equipped with damper, are investigated. The results of the study highlight the effectiveness of the LCC-based optimal design process for achieving the desired balance between initial construction cost and seismic losses. Additionally, the study adds to the literature by examining the performance difference between an optimal designed frame without damper and an existing frame optimally equipped with damper, and the performance difference between an existing frame optimally equipped with damper and a new frame optimized simultaneously with damper. The results show that adding dampers to properly designed existing structures can sufficiently improve performance without the need to design a new building with damper.

Keywords

Seismic design; Life-cycle cost; FEMA P-58; Optimization; Yielding metallic device

[1] Corresponding author, E-mail: a-karam@um.ac.ir

1- Introduction

The use of yielding metallic devices, such as hysteretic dampers, has become a popular method for improving the seismic performance of building structures. These devices can effectively dissipate a large amount of vibration energy during earthquakes, which helps to reduce the overall damage to the building structure. However, it is important to carefully consider the potential impact of these dampers on non-structural components, as they may increase the acceleration response and lead to damage of these components. Therefore, it is crucial to optimize the design of these dampers to ensure their stiffness and energy-absorbing features are appropriate for the specific building structure. By doing so, the main structural components can be optimized for their required stiffnesses and load-bearing features, which can further enhance the overall seismic performance of the building structure [1].

Destructive earthquakes in recent years have demonstrated that structures designed and built to comply with prescriptive codes have suffered significant economic losses and extended downtime [2,3]. Although meeting the minimum building code requirements can prevent structural collapse during earthquakes, it may not guarantee the expected level of building performance [4]. Performance-based earthquake engineering (PBEE) has emerged as a promising approach to address the limitations of conventional building codes in ensuring the safety and functionality of structures under seismic hazards [5]. PBEE procedures can provide a higher level of confidence in predicting building performance under seismic hazards, reducing uncertainty and financial losses. FEMA P-58 [6] provides a state-of-the-art performance-based evaluation and design methodology, widely recognized for its comprehensive and probabilistic approach to predict the seismic consequences. Developed by researchers at the Pacific Earthquake Engineering Research (PEER) Center [7–9], it consists of four analysis components: hazard analysis, structural analysis, damage analysis, and loss analysis, mathematically related by the total probability theorem. While FEMA P-58 procedure has been employed in several research studies in recent years, its application to evaluate a large set of design alternatives remains challenging due to the high computational demand required for its execution [10,11].

The optimal balance between initial construction costs and seismic consequences is a crucial issue in the design of structures. However, identifying the necessary characteristics of structural system components to achieve this balance is a challenging task. Extensive research has been conducted to identify an optimum balance between construction cost and seismic consequences for controlled [12–16] and non-controlled [17–20][21] buildings. While numerous studies have focused on the performance-based optimum design of controlled buildings with energy dissipating devices, these studies are often limited by one or more of the following factors: (1) reliance on approximate methods of structural modeling or seismic response analysis [16,22–25], (2) use of approximate loss assessment approaches, such as ATC-13 [26] or HAZUS [27] procedures, to evaluate the seismic losses [14,16,22,25,28,29], and (3) high computational efforts required to perform the design optimization, which make the design procedure impractical [13–16,30,31].

This study aims to investigate and compare different building design scenarios with and without metallic yielding dampers using a life-cycle cost (LCC)-based optimal design process. The objective is to minimize the LCC as the design criteria. The LCC includes the construction cost and loss of the lifetime seismic consequences [17][22]. Previous related studies despite having one of the mentioned threefold limitations, have focused on optimizing existing building frames with energy dissipation devices and comparing their performance with and without dampers [14,16,23–25,28,30,31]. This study adds to previous research by examining two new issues: 1) the difference in performance between an optimal designed frame without damper and an existing frame optimally equipped with damper, and 2) the difference in performance between an existing frame optimally equipped with damper and a new frame optimized simultaneously with damper. The study uses an efficient response analysis tool to address the computational challenges of simultaneous design optimization. This study employs the endurance time (ET) analysis [32] for structural response analysis and comprehensive FEMA P-58 procedure [33] for seismic loss assessment within the design process. This approach addresses the limitations of existing literature and ensures a more comprehensive analysis [34]. Additionally, the design constraints are formulated based on the specifications of the design code [35].

Two steel moment-resisting frame (MRF) buildings, with four and eight stories, are investigated. Each building is designed using four different approaches, including:

1. Typical Code-based design of an existing MRF without damper
2. Optimal LCC-based design of a new MRF without damper
3. Optimal LCC-based design of an existing MRF equipped with damper
4. Optimal LCC-based design of a new MRF equipped with damper

While previous studies have focused on comparing the first and third design approaches [14,16,23–25,28,30,31], this study adds to the literature by addressing the second and fourth design approaches. In the fourth scenario, the number of design variables increases significantly, leading to a more complex optimization problem. This complexity may be one reason why simultaneous optimization of both structure and damper characteristics has been less frequently investigated in past studies. Nevertheless, the use of the ET analysis [32] in this study makes it easier to implement optimization procedures by considerably reducing computational efforts while still reliably evaluating the seismic performance.

The rest of this paper are structured as follows: Section 2 provides a comprehensive overview of the methodology employed in this study. Section 3 presents the models and assumptions of the case study. Section 4 outlines the optimization problems, presents the properties of the design outcomes, and provides an in-depth analysis of the outcomes associated with various design approaches. Finally, Section 5 offers concluding remarks to summarize the findings of this study.

2- Design Methodology

2-1 FEMA P-58 Procedure Overview

This research utilizes the FEMA P-58 procedure [33] to estimate the seismic consequences of the considered structures. FEMA P-58 uses multiple performance metrics, such as repair cost, downtime, injuries, and casualties, to assess building performance under earthquake events. Three types of assessments are available, including intensity-based, scenario-based, and time-based. Intensity-based evaluates the building performance subject to a specific earthquake intensity, scenario-based examines the performance subject to a specific earthquake scenario, while time-based considers the probability of all possible earthquakes occurring over a specified period. More precisely, the time-based assessment evaluates the probable building performance over a specified time period, weighted by the frequency of occurrence of intensity-based assessments [11]. FEMA P-58 performance evaluation include five parts, which are briefly described as follows.

2-1-1 Define Building Performance Model

The building performance model is constructed by categorizing vulnerable building components into fragility groups with specific fragility specifications. Fragility models are statistical models that represent the probability of structural damage as a function of a single demand parameter. Typically, these models assume a lognormal distribution for the demand parameter. Fragility groups experiencing similar earthquake demands are then classified into performance groups based on the typical quantity of structural components and non-structural contents. Lastly, a time-dependent population model is defined based on occupancy, time, day, and month.

2-1-2 Define Earthquake Hazard

In the time-based assessment approach, the seismic hazards associated with earthquakes are defined through the use of seismic hazard curves [36]. These measures are employed to describe the intensity of earthquake shaking at selected annual rate of exceedance. The site-specific hazard curves are used to generate a set of earthquake hazard intensities. Here, 30 intensity levels are selected that cover a meaningful range of occurrence probabilities. The corresponding spectral response accelerations at each intensity are then used in the performance assessment analyses.

2-1-3 Evaluate Structural Response

Structural analysis is a tool used in evaluating how buildings respond to earthquake shaking, with the aim of producing median values of structural response parameters along with their corresponding dispersions. Such parameters are then correlated with the extent of damage. Main response parameters include peak interstory drift ratio, peak floor acceleration, and residual drift ratio. In this regard, FEMA P-58 outlines two alternative analysis procedures, namely simplified analysis and nonlinear response history analysis, that can be used to estimate median and dispersion of the demand parameters. However, in this study, the ET analysis [32]

is utilized to assess the structural response parameters. Further explanations of the concept and procedure of the ET analysis are provided later in this paper.

2-1-4 Evaluate Collapse Fragility

In order to assess the injuries and casualties due to building collapse, it is essential to establish the likelihood of the structural collapse based on the intensity of the earthquake, as well as the potential modes of collapse, such as partial or complete. To quantify these parameters, FEMA P-58 employs collapse fragility functions, which express the probability of collapse as a lognormal distribution. The median collapse capacity, denoted by $S_a(T)$, and the dispersion, represented by β, are the factors that generate the collapse fragility function.

2-1-5 Calculate Performance

FEMA P-58 employs a Monte Carlo simulation procedure [9] to incorporate the potential uncertainties in the predicted performance. Figure 1 illustrates the process of calculating the seismic performance based on FEMA P-58. In this regard, for each seismic hazard level, a great number of realizations should be generated. For each realization, a set of possible performance outcomes is simulated. First, it is checked whether the building collapsed or not. For this purpose, a comparison is made between a stochastic number within the range of 0 to 1 and the collapse probability derived from the collapse fragility curve that corresponds to the seismic intensity of the realization. If the building collapses, the seismic consequences (such as repair costs) are presumed to be equivalent to the replacement-related values, and the building is classified as unsafe. The fatalities due to building collapse is calculated by utilizing the occupancy population model and the potential modes of collapse. In cases where the building remains stable after the event, an evaluation is carried out to determine the feasibility of repairing the structure. This assessment considers factors such as the peak residual drift ratio and employs the fragility model of building repairability. In the event that a building is deemed irreparable, it is assumed that the seismic consequences will be equivalent to the cost of replacing the structure, thereby classifying it as unsafe. On the other hand, if the building remains stable and is determined as repairable, simulated demands are used to assess the damage state for all structural and non-structural vulnerable components. The damage states are determined using a random number generation process, and the corresponding consequences are then calculated based on the identified damage states. Finally, for each seismic intensity level, the cumulative distribution of each consequence is established by arranging the results obtained from all iterations in either an increasing or decreasing order.

The total probability theorem can be used to assess the expected annual loss (EAL) due to all seismic intensities as follows:

$$EAL = \int_{im} \mathrm{E}\left[L \mid IM = im\right] \mathrm{d}\lambda(im) \tag{1}$$

where, $\mathrm{E}[L \mid IM = im]$ refers to the expected seismic consequence (e.g., downtime) given the seismic intensity measure *im*, and $\mathrm{d}\lambda(im)$ represents the annual frequency of intensity measure *im*, as determined by the application of the hazard curve.

The computation of the lifetime loss (LL) can be evaluated by employing the equation recommended by [17] for each consequence.

$$LL = EAL\frac{1}{r}\left(1-e^{-rT}\right) \tag{2}$$

where, r represents the annualized discounting rate, while T corresponds to the lifespan of the building. In this study, a discounting rate of 0.03 and a building lifespan of 50 years have been adopted as assumed values.

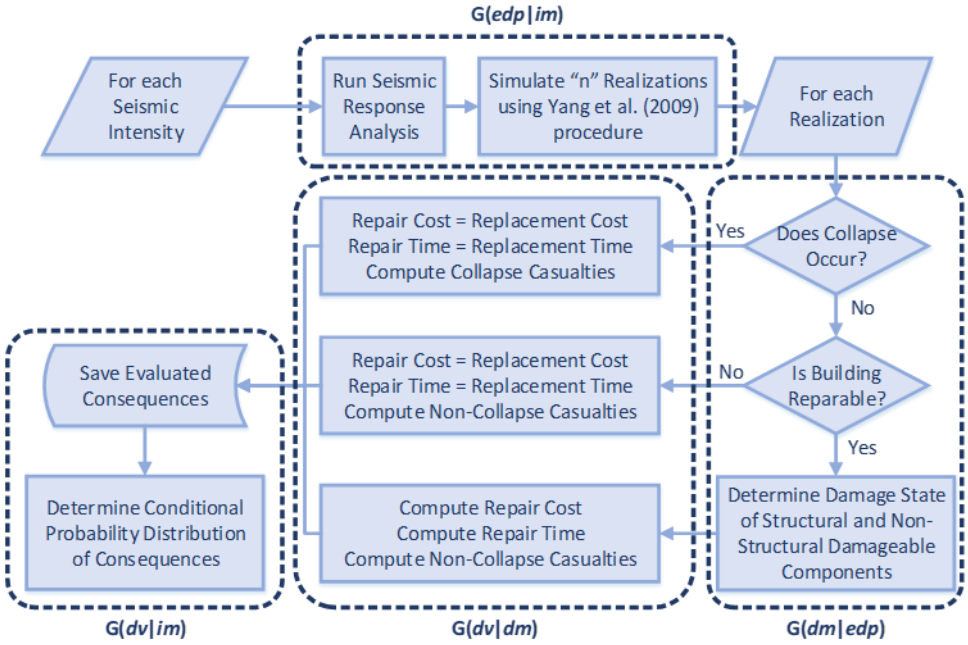

Figure 1. The process of calculating the seismic performance based on FEMA P-58 [33]

2-2 Endurance Time Analysis

The Endurance Time (ET) Analysis [32] is a powerful dynamic analysis technique for seismic assessment of structures, designed to reduce the computational burden of conventional dynamic analysis methods. The method uses a set of pre-designed artificial accelerograms known as Endurance Time Excitation Functions (ETEFs), as the excitation inputs [37]. These ETEFs are ramp-like, with their amplitude gradually increasing over time, and are produced using optimization techniques and the concept of matching response spectra. By conducting a single response-history analysis utilizing the ETEFs, the method can predict the results of response-history analyses under real ground motions scaled at entire seismic intensities. The ET Analysis is advantageous because it can provide reliable estimates of seismic performance while demanding significantly fewer computational resources than traditional response-history analyses. The ET Analysis provides a practical framework for structural optimization, which enables the use of optimization tools in the design process by considerably reducing the computational efforts associated with structural analysis procedures.

Many studies have shown the effectiveness of the ET analysis in evaluating the seismic performance of structures. For example, the ET analysis is well-suited for evaluating the

seismic response of various structures, including concrete and steel buildings [10,38], systems controlled with frictional [39], yielding [40], viscous , and tuned mass [41] dampers, isolated systems with LRB [29] and TFPB [42], long-span bridges [43], arch dams [44], and double-deck viaducts [45].

Figure 2 depicts the procedure of estimating engineering demand parameters (EDPs) using the ET analysis, outlining the key steps briefly. For, more documentation about the concept of ET analysis, available produced ETEFs, and a detailed application procedure, please refer to the ET analysis website [46].

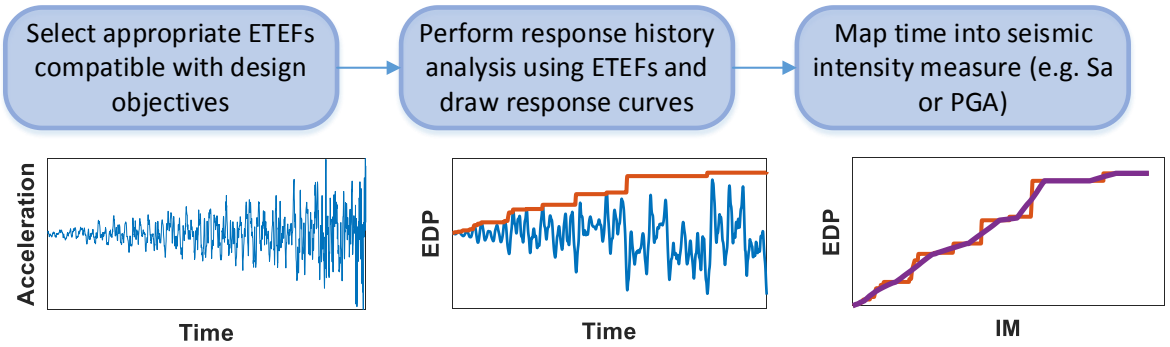

Figure 2. The overview of evaluating the EDPs through the ET analysis [34]

2-3 Optimization Problem

The process of designing a structure involves solving an optimization problem. This problem involves minimizing the total cost of the structure, which includes both the initial construction cost and the cost of maintaining it throughout its lifetime. The design variables, which are the characteristics of the structure, must be determined in an optimal manner during the design process. Additionally, the optimization constraints include meeting the code specifications. The mathematical formulation of the optimization problem is presented below:

$$\begin{aligned} &\text{Find} && X = [x_1, x_2, ..., x_n] \\ &\text{to minimize} && C_T(X) \\ &\text{subject to} && g_j(X) \le 0 \quad j = 1, ..., k \end{aligned} \tag{3}$$

in which, X represents the vector of design variables, C_T addresses the total cost (LCC) of a given system, while the g_j refers to the constraints that should be fulfilled. The next sub-sections will cover various parts of the optimization problem.

2-3-1 Objective Function

The objective function to minimize in this study is the total cost, which encompasses both the long-term seismic consequences and the construction cost. In order to focus solely on the variables related to the design, constant costs that are independent of design variables, such as maintenance and operation costs, as well as non-structural components and building land price, are excluded from the objective function [17]. The construction cost is evaluated based on the weight of the structural frame, which serves as an indicator. The unit cost of structural steel weight, which includes material, transportation, operation, and labor, is set at 6.0 $/kg, as reported in [11]. This cost is adjusted for the year 2022 in Los Angeles, CA, according to data

from RS Means [47]. A supplementary 15% surcharge is included in the unit cost to accommodate for the expenses related to steel connections.

The seismic consequences, including repair cost, downtime, injury, and casualty, are considered as losses. To determine the financial impact of these losses, appropriate multipliers are used to convert each component into an equivalent financial cost. The unit cost of casualty is defined based on value of statistical life and set at $\$10.2\times10^6$ million per person as suggested by [48]. The unit cost of injury (moderate) is set at $480,000 per person, which is assumed to be 4.7% of the casualty loss based on [49]. The loss of downtime is calculated as the sum of the relocation loss and the rental rate, with a value of $130.0 per month per square meter adopted from [11]. The cost function is determined using Eq. (4):

$$C_T = C_{in} + C_{rep} + C_{down} + C_{inj} + C_{fat} \tag{4}$$

where, C_{in} represents the initial cost of construction, and C_{rep}, C_{down}, C_{inj}, and C_{fat} denote the lifetime costs associated with repair, downtime, injury, and fatality, respectively.

2-3-2 Constraints

The optimization problem in this context is constrained by prescriptive code requirements. Specifically, the design constraints include the allowable interstory drift ratio, the demand-to-capacity ratio for beams and columns, and the requirement for strong columns and weak beams. These constraints are expressed as expressed by Eq. (5) [50] and should assure Eq. (3).

$$g_1 = \frac{\Delta}{\Delta_{allowable}} - 1 \qquad g_2 = \frac{\sum M_{pc}}{\sum M_{pb}} - 1 \qquad g_3 = \frac{R_u}{\varphi R_n} - 1 \tag{5}$$

in which, Δ represents the peak interstory drift ratio, while $\Delta_{allowable}$ represents the allowable threshold of interstory drift ratio. M_{pb} and M_{pc} refer to flexural strengths of the beams and columns, respectively. R_u denotes the member demand, and φR_n represents the member capacity.

2-3-3 Design Procedure

The Particle Swarm Optimization (PSO) algorithm [51] is utilized in this study to identify the optimal solution. PSO is a metaheuristic optimization algorithm that does not rely on gradient information or pre-defined starting points to find the global optimum solution. Its simplicity in computer implementation and suitability for parallel computing make it an attractive choice for solving complex optimization problems. By employing an evolutionary search approach from one population to the next, PSO enables the identification of structural designs that are close to the global minimum.

The initial step is to generate a set of preliminary design alternatives. This is achieved through a random generation of design variables within the allowable range. Subsequently, each design alternative is evaluated against the objective function and the constraints. The algorithm's stopping criteria are then checked to determine if they have been met. If the criteria are not assured, a new set of design alternatives is produced using the algorithm rules, and the evaluations are repeated. The iterative procedure persists until the predefined stopping

conditions are satisfied. It is essential to note that the use of appropriate mathematical formulations and adherence to the specified stopping criteria are critical in ensuring the integrity and reliability of the design optimization process.

The evaluation of design alternatives begins with a thorough examination of the code requirements. This involves the development of a linear analytical model, followed by conducting the response-spectrum analysis method. Subsequently, the constraints are assessed based on the results obtained from the analysis. These constraints are then incorporated into the objective cost through the application of a penalty factor. In addition, the initial cost is evaluated based on the properties of the structural frame. To estimate the seismic losses, a nonlinear structural model is prepared initially. This is followed by conducting ET analysis to evaluate the EDPs. Then, the consequences are determined employing the FEMA P-58 procedure, as outlined in Section 2.1. Finally, the LCC is calculated using Eq. (4).

3- Modeling and Assumptions

3-1 Structural Model

For the present research study, two special steel MRFs of four and eight stories are selected from the NIST report [52]. The chosen MRFs are equipped with a perimeter steel lateral-resisting system in both plan directions and have a plan with dimensions of 30 m by 43 m, as illustrated in Figure 3. The lateral loads are supported by two three-bay MRFs in each direction, while the remaining frames support the gravity loads. The story height is assumed 4.6m for the first story, and 4.1m for other stories. The structural plan is symmetrical and regular in the plan [52]. Therefore, the MRF of the shorter plan direction is chosen for the time-history analysis, given a higher aspect ratio. This MRF is assigned half the seismic mass of the building. Figure 4 provides an elevation view of the selected MRFs. The structures are located in Los Angeles, CA. The soil in the location is classified as type D, and the seismic design category assigned to the buildings is D_{max}, based on ASCE 7-22 [53]. The buildings are designed for office occupancy, and the yield strength of the steel members is 345 MPa. The assumed dead load is 440 kg/m^2 for all levels, while the assumed live load is 240 and 100 kg/m^2 for the typical floors and roof, respectively.

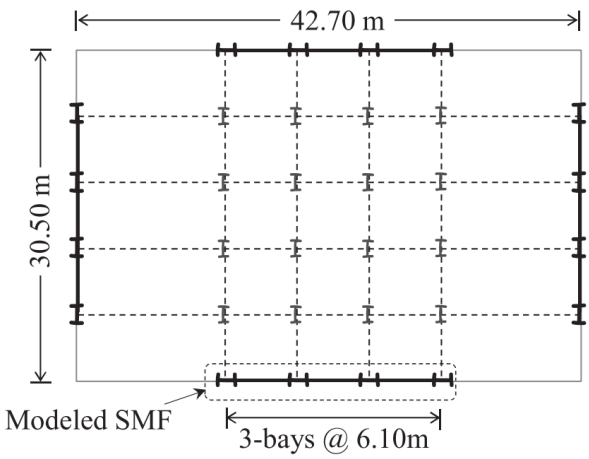

Figure 3. Plan configuration of the selected buildings [52]

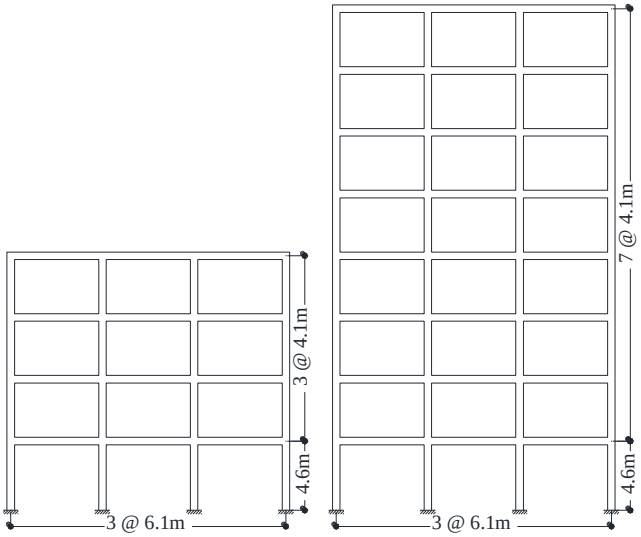

Figure 4. Elevation view of the modeled MRFs

3-2 Supplementary Device Characteristics

The behavior of supplemental devices plays a crucial role in determining the overall stiffness and strength of a system, which, in turn, affects the seismic behavior and the corresponding consequences during seismic events. Optimizing the system performance and minimizing the LCC is essential, and to achieve this, it is necessary to identify the device parameters that have the most significant impact on stiffness and yielding characteristics. A schematic representation of a structure with yielding metallic devices can be constructed using three essential elements: structural members, supplementary device, and brace elements that provide support and connection to the primary structure. The supplementary device and brace elements are arranged in a series configuration, while the brace-device assembly is arranged in parallel with the story structural members. The resultant stiffness of the brace-device assembly, denoted as k_{DB}, can be mathematically represented as follows [14]:

$$k_{DB} = \frac{1}{1/k_D + 1/k_B} = \frac{k_D}{1 + 1/r_{BD}} \tag{6}$$

in which, k_D and k_B respectively express the stiffness of the yielding damper and the supporting brace. The ratio of the brace to the device stiffness, r_{BD}, is calculated as $r_{BD} = k_B/k_D$. The total story stiffness of the structural system can be determined by combining the stiffness of the device-brace assembly with the interstory stiffness. Previous studies [22,54] revealed that r_{BD} has a negligible effect on the system behavior. Therefore, it is assumed that ratio of the brace to the device stiffness remains constant as $r_{BD} = 2$. This assumption enables the brace-device assembly stiffness, as well as the structural system stiffness, to be expressed based on the device stiffness.

The stiffness and yield strength of the yielding damper are contingent upon two factors: the number of yielding plates, n_p, and their respective dimensions. The initial stiffness, k_D, the yield displacement, δ_{Dy}, and the yield capacity, P_y, for a triangular-shaped (TADAS) device element can be mathematically represented as follows [14]:

$$k_D = \frac{n_p E}{\int_0^{h_p}\int_0^x \frac{1}{I(x)}\mathrm{d}x\mathrm{d}x} = \frac{n_p E B_p t_p^3}{6H_p^3} \tag{7}$$

$$\delta_{Dy} = \frac{F_y}{E}\int_0^{H_p}\int_0^x \frac{1}{y(x)}\mathrm{d}x\mathrm{d}x = \frac{F_y H_p^2}{E t_p} \tag{8}$$

$$P_y = k_D \delta_{Dy} = \frac{n_p F_y B_p t_p^2}{6H_p} = k_{DB}\left(1+\frac{1}{r_{BD}}\right)\delta_{Dy} \tag{9}$$

where E represents the Young's modulus, F_y is the yield stress, B_p is the plate width, H_p is the plate length, t_p is the plate thickness, and δ_{Dy} indicates the yield displacement of the device.

Generally, design parameters of a TADAS device include: (1) the number of plates n_p, (2) the thickness of plates t_p, (3) width of the plates at the bottom B_p, and (4) height of the plates H_p. The number of plates per device is the most important design parameter of the TADAS system [14]. As a result, in the present study, other parameters are assumed to be fixed and the number of plates is considered as a design variable for optimization. Thus, the width and height of the plates are considered as B_p = 250mm and H_p = 400mm, respectively. Moreover, the plate thickness is chosen as t_p = 35mm.

It should be noted that the thickness is selected based on the maximum allowable plate thickness in the device. Xia and Hanson [54] suggested that the plate thickness of the yielding device should be such that the yield drift of the device is placed in the drift range of 0.0014 H–0.002 H, where H is the story height. Therefore, the limited thickness allowed for the plate is between 26 and 36mm. Additionally, Shin et al. [14] found that a greater thickness of the TADAS device plate results in better performance in terms of LCC, with the maximum thickness being the optimal thickness. Therefore, the present study considers a plate thickness of 35 mm.

The cost of implementation a TADAS system on a MRF includes the cost of TADAS assembly and its supporting braces. The cost of a single TADAS assembly can be further broken down into two component costs: the cost of the steel plates utilized in the assembly and the cost of the base on which the plates are connected and subsequently linked to the supports. Both costs can be assumed to be proportionate to the amount of material employed and can be roughly expressed as a function of plate thickness. This research paper has adopted the cost of producing the plates and base assembly from Shin et al. [14], which is based on the unit costs of \$8.5/mm for the plates and \$11.8/mm of the plate thickness for the base block. This cost incorporates the cost of materials, cutting, bolting, and fabrication, as well as other expenses such as contractor's fee, and so on. The cost of the support member can also be calculated based on the amount of material used in the brace and the unit cost of steel. For this calculation, the unit cost of steel for the brace members is adopted from RS Means [47] as \$7.5 per kilogram. It is important to note that these costs have been adjusted for the year 2022 in Los Angeles, CA, based on data from RS Means [47].

3-3 Nonlinear Analytical Model

To evaluate each design alternative, a two-dimensional nonlinear model is developed using the OpenSees environment [55]. The nonlinear behavior of structural members is modeled using the concentrated plasticity approach, suggested by NIST report [52]. Specifically, the beams and columns are simulated by a linear beam-column element that features nonlinear flexural springs at both ends [56]. The nonlinear cyclic behavior of these flexural springs is determined using regression equations that are derived from an experimental database recommended by [57,58]. Additionally, the panel zone nonlinear behavior is considered using a rotational spring and a set of rigid elements [59]. A bilinear model is used to describe the hysteretic behavior of the metallic damper, with the post-yield stiffness of steel plates defined as 1% of the initial stiffness [14,60]. To simulate the damping effect, Rayleigh damping model is employed with a damping ratio of 2.5% [61]. To address the P-Delta effects, the model includes leaning columns that are rigidly connected to the building. Figure 5 provides a visual representation of the analytical model employed here for a 4-story frame.

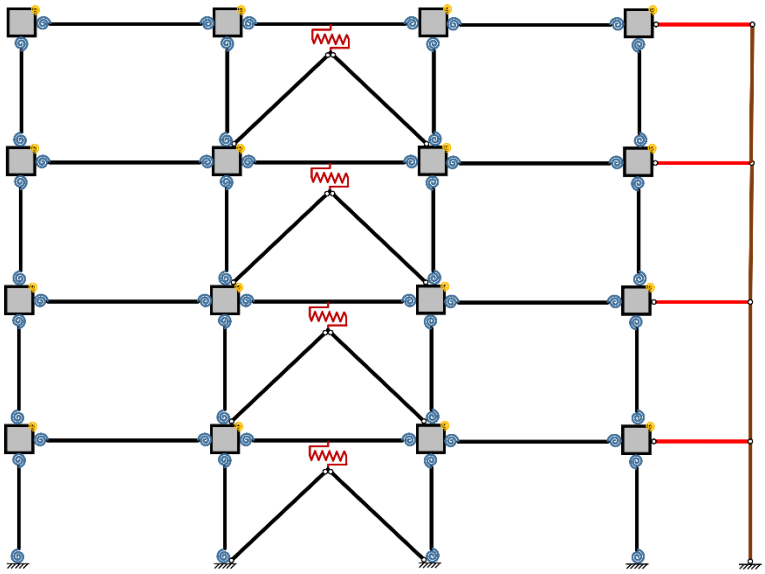

Figure 5. Schematic of the analytical model employed in this study for a 4-story frame

3-4 Loss Assessment Assumptions

This section outlines the necessary assumptions for implementation of the FEMA P-58 procedure. For commercial office buildings, the peak occupancy rate is assumed to be four occupants per 100 square meters of building area. The unit replacement cost of the building is adopted from RSMeans [47] at a value of $2450 per square meter for a conventional steel building in Los Angeles in 2022. The building replacement time is considered to be 680 and 790 days for 4- and 8-story structures, respectively, as suggested by [62]. Normative Quantity Estimation Tool established by FEMA P-58 [63] is used to determine the damageable structural and non-structural components, which are similar to those described in [34]. The fragility curves and consequence functions for each component are obtained from the fragility database of FEMA P-58 [63].

The buildings in Los Angeles, CA are situated on a soil of Site Class D. The seismic hazard curve for the site is obtained from the USGS online tool [64] and is illustrated in Figure 6. To assess potential losses, 30 seismic hazard levels are uniformly selected ranging from PGA = 0.025g to PGA = 1.525g as recommended by FEMA P-58 [33]. The lower bound indicates a hazard level with no expected loss, while the upper bound represents an infrequent earthquake occurrence with a return period of 5000 years.

The EDPs are predicted using the probabilistic ET analysis utilizing *lc* set of excitation functions [65], which is a more advanced technique compared to the conventional ET analysis. The conventional method only estimates the median EDPs and relies on judgment-based dispersion parameters for assessing uncertainties in the absence of sufficient ground motion data [10]. However, this approach is limited in its accuracy and reliability. The probabilistic ET analysis overcomes this limitation by directly predicting probabilistic seismic responses, which enables a more accurate evaluation of record-to-record variability.

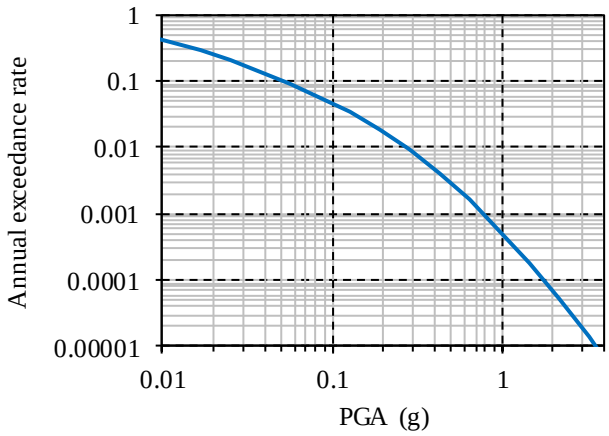

Figure 6. Hazard model of downtown Los Angeles, CA adopted from [64]

4- Design Optimization

4-1 Design Approaches

The present study, with the help of a reliable and efficient LCC-based optimal design process, aims to investigate and compare different design scenarios without and with dampers at the same time, which have not been addressed in previous studies. Previous studies mainly selected existing building frames that were commonly designed based on seismic codes and then optimized them with the help of energy dissipation devices based on LCC (or similar criteria) [14,16,23–25,28,30,31]. Then, they compared the performance of initial frame without damper and the frame with damper. The results of previous studies all confirmed the significant performance improvement of frames with damper. The current study, in addition to confirming the results of previous studies, examines two new issues.

The question may arise, what is the performance of the frame without damper if it is designed based on LCC from the beginning compared to the frame with damper based on LCC? Most other studies have also shown that if a bare frame is also designed based on LCC, its

performance will improve significantly. But it is unclear how much the addition of the damper increases the performance improvement. Also, the question may arise that during the design of the frame with damper, if at the same time the specifications of the frame are also optimally designed together with the damper, compared to the case where the damper is applied to the existing frame, how is it different in terms of performance? In the case of simultaneous design of frame and damper specifications, the computational cost increases greatly due to the significant increase in the complexity of the optimization problem. As a result, few studies in the literature have addressed this issue. In the current study, which uses ET analysis as an efficient response analysis tool, the possibility of solving such a problem becomes easier.

In this regard, two buildings, one with four stories and the other with eight stories, are investigated. Each building is designed using four different approaches, including:

1. Typical existing MRF without damper (T-MRF)
2. Optimal LCC-based design of a new MRF without damper (O-MRF)
3. Optimal LCC-based design of an existing MRF equipped with damper (T-MRF + O-TADAS)
4. Optimal LCC-based design of a new MRF equipped with damper (O-MRF + O-TADAS)

Previous studies have primarily focused on comparing the first and third design approaches, despite having one of the mentioned threefold limitations. In contrast, this study addresses two additional problems including the second and fourth design approaches.

Details of Design Outcomes

Table 1 presents the list of sections selected for the design of the beam and column members of the frames examined in this study. According to the table, W24 sections are used for columns, and W18, W24 and W30 sections are used for beams.

For the first design approach, which aims to design a typical MRF without dampers, this study selected the 4- and 8-story RSA-D_{max} MRFs from the NIST report [52]. These frames serve as suitable examples of practitioner-designed buildings and are therefore representative of current industry practices. Table 2 and Table 3 summarize the structural properties of the beams and columns for these frames, which are referred here as typical MRFs (T-MRFs). For other design approaches, optimization has been conducted. Table 2 and Table 3 also provides the optimal structural properties resulting from each approach for the 4- and 8-story frames, respectively.

Table 4 provides the natural period of the design outcomes. The natural period can be an indicator of the overall lateral stiffness of the structure. According to the table, the natural period of the LCC-based design outcomes in both 4-story and 8-story buildings is lower than the code-based T-MRF outcome. This implies that to minimize the LCC, it is necessary to increase the structural lateral stiffness.

Table 1. List of sections selected for the design of the beam and column members of examined frames

Element Type	Considered List of Available Sections							
Beams	W18X35	W18X40	W18X46	W24X55	W24X62	W24X68	W24X76	W24X84
	W24X94	W30X90	W30X99	W30X108	W30X116	W30X124	W30X132	W30X148
Columns	W24X55	W24X62	W24X68	W24X76	W24X84	W24X94	W24X103	W24X104
	W24X117	W24X131	W24X146	W24X162	W24X176	W24X192	W24X207	W24X229
	W24X250	W24X279	W24X306	W24X335	W24X370			

Table 2. Properties of the 4-story designed frame relevant to various design methods

Design Approach	Story No.	Beam	Exterior Column	Interior Column	Damper
		Section	Section	Section	Number of plates
T-MRF	1 & 2	W21X73	W24X103	W24X103	-
	3 & 4	W21X57	W24X62	W24X62	-
O-MRF	1 & 2	W30X124	W24X279	W24X306	-
	3 & 4	W30X148	W24X162	W24X306	-
T-MRF + O-TADAS	1 & 2	W21X73	W24X103	W24X103	14 & 48
	3 & 4	W21X57	W24X62	W24X62	28 & 48
O-MRF + O-TADAS	1 & 2	W30X116	W24X229	W24X103	48 & 38
	3 & 4	W30X108	W24X370	W24X176	45 & 48

Table 3. Properties of the 8-story designed frame relevant to various design methods

Design Approach	Story No.	Beam	Exterior Column	Interior Column	Damper
		Section	Section	Section	Number of plates
T-MRF	1 & 2	W30X116	W24X131	W24X162	-
	3 & 4	W27X94	W24X131	W24X162	-
	5 & 6	W24X84	W24X131	W24X131	-
	7 & 8	W21X68	W24X94	W24X94	-
O-MRF	1 & 2	W30X99	W24X370	W24X370	-
	3 & 4	W30X148	W24X279	W24X335	-
	5 & 6	W30X148	W24X279	W24X306	-
	7 & 8	W30X148	W24X162	W24X306	-
T-MRF + O-TADAS	1 & 2	W30X116	W24X131	W24X162	34 & 36
	3 & 4	W27X94	W24X131	W24X162	12 & 20
	5 & 6	W24X84	W24X131	W24X131	26 & 44
	7 & 8	W21X68	W24X94	W24X94	30 & 48
O-MRF + O-TADAS	1 & 2	W24X76	W24X306	W24X306	3 & 30
	3 & 4	W24X84	W24X250	W24X306	21 & 31
	5 & 6	W30X132	W24X176	W24X207	39 & 39
	7 & 8	W30X124	W24X131	W24X192	39 & 39

Table 4. The building natural period of the design outcomes

Design Approach	4-story	8-story
T-MRF	1.60 sec	2.16 sec
O-MRF	0.82 sec	1.57 sec
T-MRF + O-TADAS	0.94 sec	1.64 sec
O-MRF + O-TADAS	0.60 sec	1.57 sec

4-2 Evaluation of Design Outcomes

Figure 7 provides a comparison of the LCC components associated with different design outcomes. The components provided in this figure include frame construction cost, repair cost, and losses due to downtime, injury, and casualty. The considered four design approaches are labeled as #1 to #4. Design #1 refers to the T-MRF approach and involves typically designing a building based on seismic code specifications. Design #2, the O-MRF approach, aims to optimize the frame design without damper based on the LCC. Method #3, the T-MRF + O-TADAS approach, involves adding damper to an existing building and optimizing the damper specifications based on the LCC. Finally, Design #4, the O-MRF + O-TADAS approach, involves designing a new building with damper so that both the frame and damper characteristics are simultaneously optimized.

As seen in Figure 7, all LCC-based design outcomes have significantly better performance than code-based outcomes, highlighting the importance of using the LCC-based design procedures. For instance, the LCC for Design #1 is, on average, 155% of the building replacement cost. On the other hand, the LCC for Designs #2, #3, and #4 is, on average, equal to 133%, 127%, and 126% of the replacement cost, respectively.

By examining Design #2, which aims to LCC-based design of a new perimeter MRF without damper, it is apparent that the overall performance is satisfactory in terms of total cost. Compared to Design #1, Design #2 resulted in a cost reduction of 26.9% of the replacement cost for the 4-story building and 15.7% of the replacement cost for the 8-story building. These cost reductions correspond to cost savings of $3,430,000 and $4,000,000, respectively. However, this saving has been achieved through an increase in construction cost, which is, on average, 4.4% of the building replacement cost. In contrast, Design #3, which optimally adds dampers to the existing frame, with only a 0.4% increase in construction cost, resulted in a total cost reduction equivalent to 34.0% of the replacement cost for the 4-story building and 21.7% of the replacement cost for the 8-story building. On the other hand, Design #4 has the best performance in terms of total cost. However, Design #4 also requires an increase in the construction cost of about 3.6% to provide the minimum total cost.

By comparing Designs #3 and #4, Design #4 has a marginally lower LCC value. The difference is only 0.7% and 1.0% of building replacement cost for the 4- and 8-story structures, respectively. On the other hand, Design #4 increases seismic frame construction costs by about 3.6% of the building replacement cost compared to Design #1. Such a high increase in construction costs may reduce the motivation of decision-makers to use LCC-based

approaches. In contrast, Design #3 effectively improves LCC by marginally increasing frame construction costs by about 0.4% of the replacement cost and reducing LCC by 27.8% of replacement cost, on average. It can be concluded that adding dampers to properly designed existing structures can sufficiently improve performance without the need to design a new building with damper.

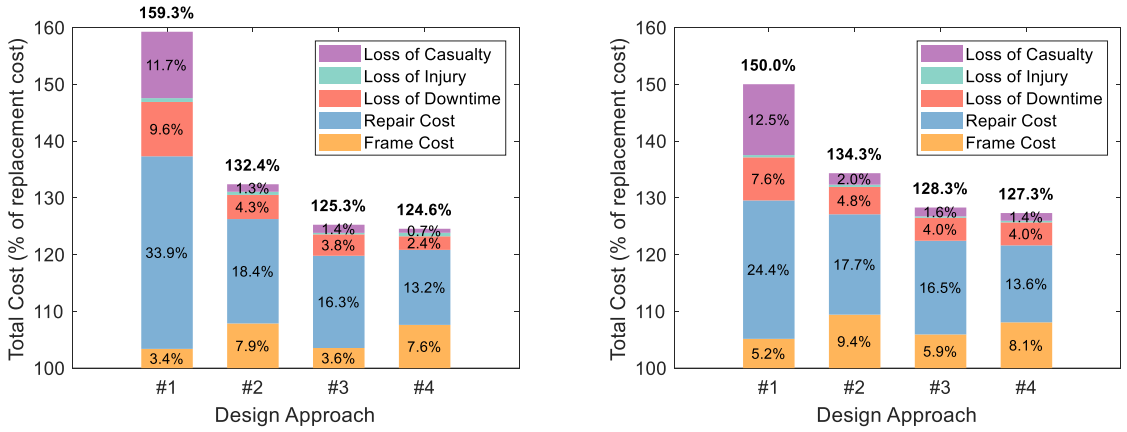

(a) (b)

Figure 7. Comparison of the LCC components of the designed structures (a) 4-story and (b) 8-story

Figure 8 and Figure 9 compare the EDPs for the outcomes of different design approaches, specifically the peak interstory drift ratio and peak floor acceleration for the 4- and 8-story buildings. Upon examining these figures, it can be seen that Designs #2 and #4 exhibit similar seismic behavior, with less interstory drift ratio and more floor acceleration than Designs #1 and #3. Considering Table 4, the increase in floor acceleration in these two design approaches can be attributed to the increase in stiffness which leads to gain more acceleration from earthquake excitation. As a result, the drift-sensitive damageable components will experience more damage and acceleration-sensitive damageable components will experience less. On the other hand, Design #3 follows a different seismic behavior. This design approach leads to less drift, while its acceleration has not increased. The lack of acceleration increase in Design #3 can be attributed to the increase in damping through the yielding of metallic dampers, which counteracts the acceleration increase caused by the stiffness increase.

However, the displacement of Design #3 increases at a higher rate starting from an intensity of about PGA = 0.9g (return period of 1450 years). At an average intensity of 1.05g, its performance becomes worse than the performance of the conventional code-based structure. The reason for this issue is the failure of the structural members that support the damper. These members are designed to carry the seismic and gravity loads of the frame without dampers. Adding the damper and brace system increases the local stiffness, leading to higher forces in the frame components adjacent to the damper. In Design #4, the frame specifications are optimized simultaneously with the damper, preventing this performance weakness. Therefore, it is suggested to check the failure of the frame components under moderate to severe earthquakes when adding dampers to the existing frame. However, in this example, the earthquakes of this intensity are unlikely to occur, and the expected loss from this performance weakness is not significant enough to question the overall performance of Design #3.

Figure 10 compares the collapse fragility curves for the outcomes of different design methods. Moreover, Table 5 presents the collapse probability of the design outcomes under design basis earthquake (DBE) and maximum considered earthquake (MCE) hazard levels. It can be seen that the LCC-based design approaches show almost similar collapse performance and significantly increase the collapse capacity compared to Design #1. The collapse probability of Design #1 under DBE and MCE hazards is about 9% and 27%, respectively. In contrast, the LCC-based designs have a collapse probability of less than 1% and 5% under DBE and MCE hazards, respectively. It can be seen that while Design #4 exhibits the best collapse performance, its superiority over Designs #2 and #3 is marginal.

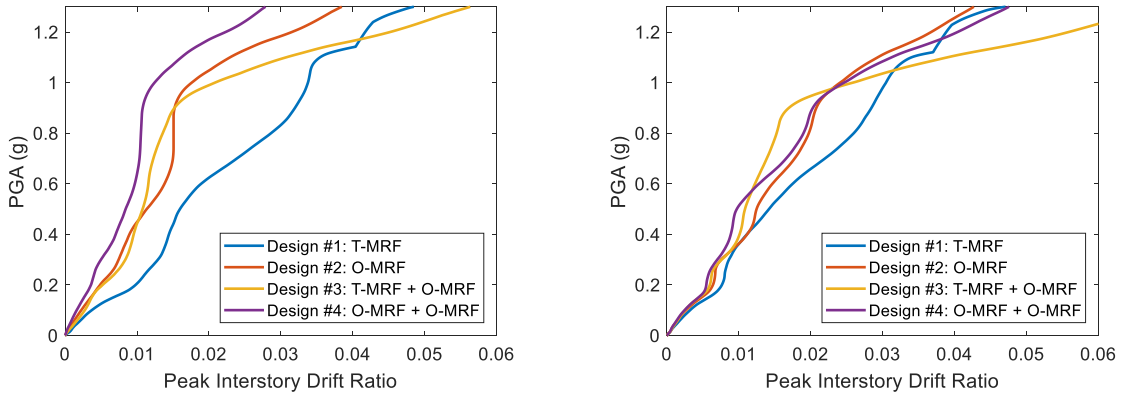

(a) (b)

Figure 8. The peak interstory drift ratio of the designed outcomes (a) 4-story and (b) 8-story

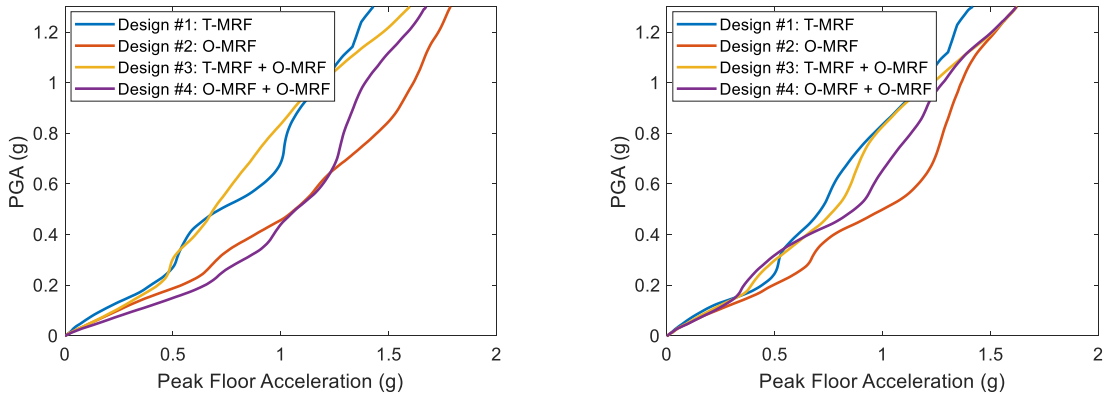

(a) (b)

Figure 9. The peak floor acceleration of the designed outcomes (a) 4-story and (b) 8-story

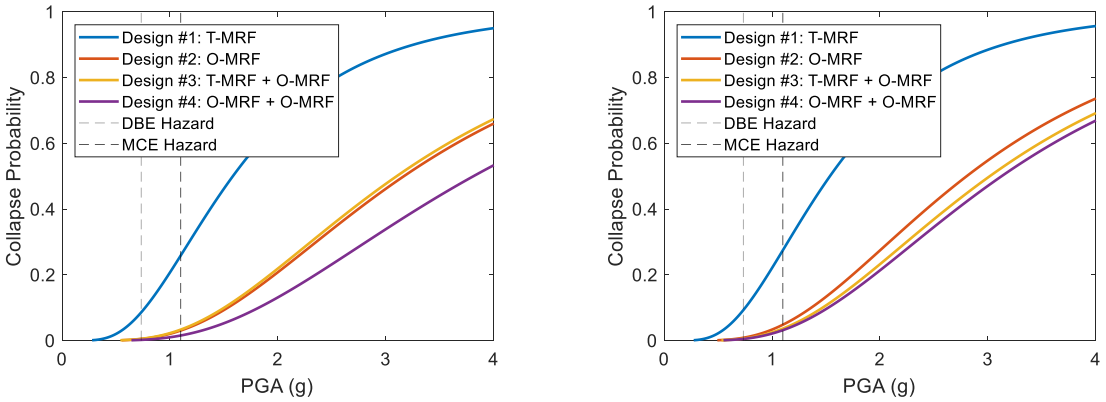

Figure 10. Collapse fragility curve of the designed outcomes (a) 4-story and (b) 8-story

Table 5. The collapse probability of the design outcomes at DBE and MCE hazard levels

Design ID	Design Approach	Collapse Probability	
		DBE Hazard	MCE Hazard
4-story			
Design #1	T-MRF	8.6%	25.9%
Design #2	O-MRF	0.5%	3.1%
Design #3	T-MRF + O-TADAS	0.5%	3.4%
Design #4	O-MRF + O-TADAS	0.2%	1.6%
8-story			
Design #1	T-MRF	9.3%	27.5%
Design #2	O-MRF	0.9%	4.8%
Design #3	T-MRF + O-TADAS	0.6%	3.6%
Design #4	O-MRF + O-TADAS	0.5%	3.2%

Figure 11 shows the seismic consequences for 8-story design outcomes as a function of the seismic intensity level. The consequences include damage cost ratio, downtime, injury, and casualty. Damage cost ratio is defined as the ratio of repair cost to the building replacement cost. Additionally, Table 6 provides the seismic loss components for the design outcomes under the DBE hazard occurrence. As seen, all design outcomes experience significant damage under the DBE and MCE hazard levels. For instance, for the 4-story frame under a DBE hazard, the code-based design outcome has a damage ratio of 55%, while the LCC-based outcomes have a damage ratio of about 40% without damper and about 33% on average with dampers. At extremely severe hazard level with a return period of 5000 years, all design outcomes converge to a damage ratio of one. In other words, at this hazard level, the damage is so extensive that the building would need to be replaced with a similar one. Furthermore, it can be seen that LCC-based design outcomes reduce downtime loss to a more significant extent. For example, under the DBE hazard, the average downtime for Design #1 is about 330 days, while it is around 100 days on average for Design #3.

It can be seen that injuries are similar among all design outcomes. It should be noted that injuries do not have a significant impact on LCC, as can be seen in Figure 5. It is evident that the casualty rate of the typical code-based building (Design #1) is considerably more than that of the LCC-based design outcomes. The casualty loss is mainly due to the collapse of the structure. As a result, since code-based design outcomes have a higher probability of collapse, greater casualties are also predicted. According to Table 6, the expected casualty loss under the DBE hazard in the LCC-based outcomes has been reduced by 90% compared to the code-based outcomes.

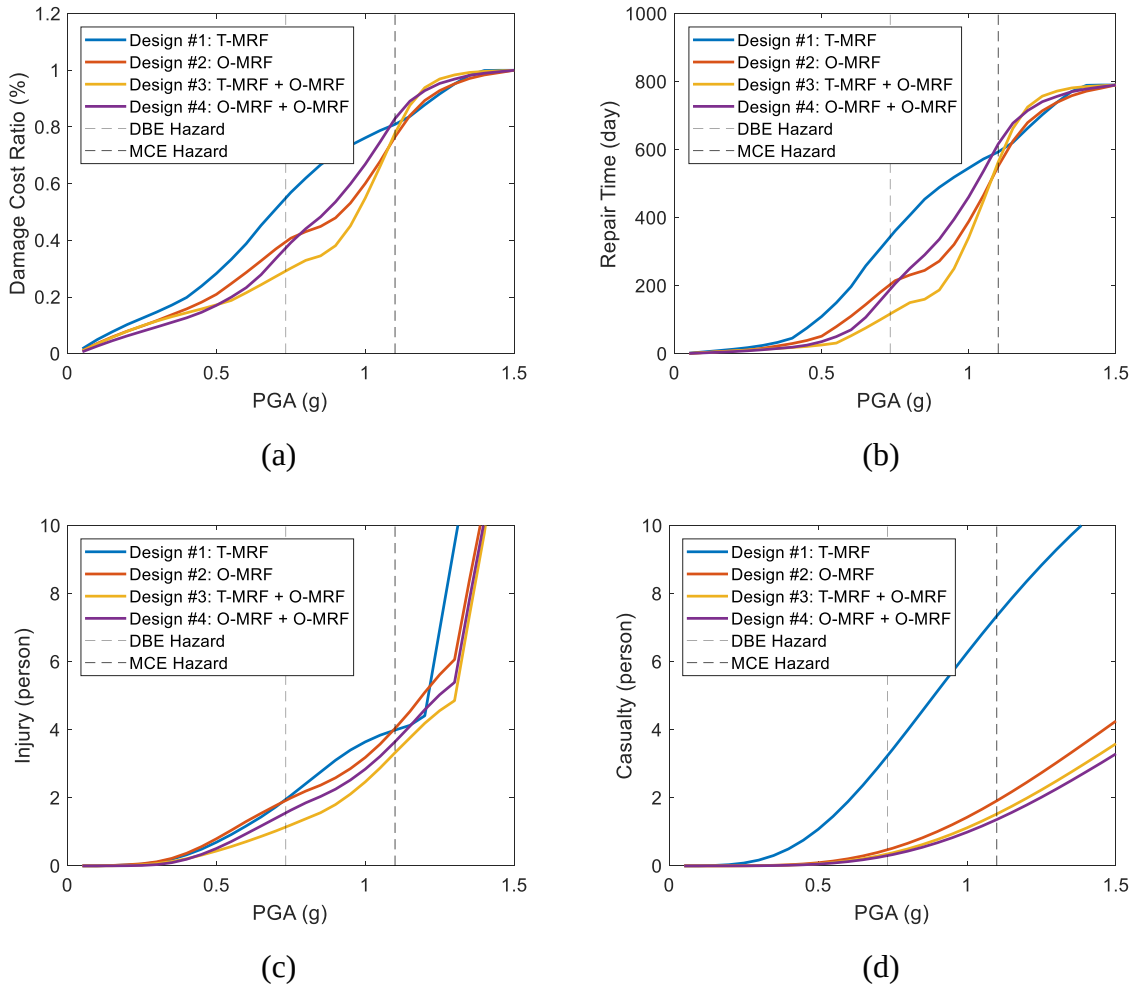

Figure 11. Seismic consequences as a function of seismic intensity for the 8-story structure (a) damage cost ratio, (b) downtime, (c) injury, and (d) casualty

Table 6. The seismic consequences of the design outcomes given DBE hazard level

Design ID	Design Approach	Damage Ratio (%)	Downtime (day)	Injury (person)	Casualty (person)
4-story					
Design #1	T-MRF	59.1	325	1.40	1.52
Design #2	O-MRF	36.3	140	1.25	0.15
Design #3	T-MRF + O-TADAS	27.7	90	0.55	0.16
Design #4	O-MRF + O-TADAS	23.4	37	1.05	0.07
8-story					
Design #1	T-MRF	54.9	343	1.95	3.25
Design #2	O-MRF	39.9	203	1.91	0.46
Design #3	T-MRF + O-TADAS	29.2	117	1.15	0.35
Design #4	O-MRF + O-TADAS	37.5	189	1.55	0.31

5- Conclusion

This study investigated and compared different building design scenarios with and without metallic yielding dampers, using an LCC-based optimal design process. The aim was to minimize the LCC as the design criteria, which includes the construction cost and loss of the lifetime seismic consequences. The study addressed the limitations of existing literature by employing the ET analysis for structural response analysis and the comprehensive FEMA P-58 procedure for seismic loss assessment in the optimization procedure. The study considered two steel MRF buildings, with four and eight stories, designed using four different approaches.

The results showed that all LCC-based design outcomes perform significantly better than code-based outcomes. Compared to the typical code-based design approach, the LCC-based outcomes showed a 27-35% reduction in LCC for the 4-story building and a 16-23% reduction in LCC for the 8-story building. The overall performance of a new optimally designed MRF without damper was found satisfactory in terms of total cost. However, performance enhancement was achieved through a 4.4% increase in construction cost. Moreover, adding dampers to an existing building and LCC-based optimizing their specifications effectively improved LCC by marginally increasing frame construction costs and reducing LCC by 27.8% of replacement cost, on average. The findings suggest that adding dampers to properly designed existing structures can sufficiently improve performance without the need to design a new building with a damper.

The results shown that LCC-based designs have a significantly higher collapse capacity compared to code-based ones. The collapse probability of code-based outcomes under DBE and MCE hazards was about 9% and 27%, respectively. In contrast, the LCC-based designs had a collapse probability of less than 1% and 5% under DBE and MCE hazards, respectively. At an extremely severe hazard level with a return period of 5000 years, all design approaches converged to a damage ratio of one, meaning that the building would need to be replaced with a similar one.

The study concluded that optimum LCC-based retrofitting of existing buildings can be more efficient than designing a new building without dampers or even with dampers. Moreover, the LCC-based design approach can lead to significant cost savings while improving the seismic safety and resilience of structures.

6- References

[1] R.I. Skinner, J.M. Kelly, A.J. Heine, Hysteretic dampers for earthquake-resistant structures, Earthquake Engineering & Structural Dynamics. 3 (1974) 287–296.

[2] FEMA 445, Next-Generation Performance-Based Seismic Design Guidelines Program Plan for New and Existing Buildings, Federal Emergency Management Agency, Washington, DC, 2006.

[3] X. Zeng, X. Lu, T.Y. Yang, Z. Xu, Application of the FEMA-P58 methodology for regional earthquake loss prediction, Natural Hazards. 83 (2016) 177–192.

[4] C.M. Ramirez, A.B. Liel, J. Mitrani-Reiser, C.B. Haselton, A.D. Spear, J. Steiner, et al., Expected Earthquake Damage and Repair Costs in Reinforced Concrete Frame Buildings, Earthquake Engineering & Structural Dynamics. 41 (2012) 1455–1475. doi:10.1002/eqe.2216.

[5] K.A. Porter, An overview of PEER's performance-based earthquake engineering methodology, in: Proc. Ninth Int. Conf. Appl. Stat. Probab. Civ. Eng., 2003: pp. 1–8.

[6] FEMA P-58, Development of Next Generation Performance-Based Seismic Design Procedures for New and Existing Buildings, Federal Emergency Management Agency, Washington, DC, 2018.

[7] C.A. Cornell, H. Krawinkler, Progress and Challenges in Seismic Performance Assessment, PEER Center News. 3 (2000) 1–3.

[8] J. Moehle, G.G. Deierlein, A Framework Methodology for Performance-Based Earthquake Engineering, in: 13th World Conf. Earthq. Eng. August 1-6, 2004, Vancouver, BC, Canada, 2004.

[9] T.Y. Yang, J. Moehle, B. Stojadinovic, A. Der Kiureghian, Seismic Performance Evaluation of Facilities: Methodology and Implementation, Journal of Structural Engineering. 135 (2009) 1146–1154. doi:10.1061/(asce)0733-9445(2009)135:10(1146).

[10] M.C. Basim, H.E. Estekanchi, Application of Endurance Time Method in Performance-Based Optimum Design of Structures, Structural Safety. 56 (2015) 52–67. doi:10.1016/j.strusafe.2015.05.005.

[11] A. Ghasemof, M. Mirtaheri, R.K. Mohammadi, Multi-objective optimization for probabilistic performance-based design of buildings using FEMA P-58 methodology, Engineering Structures. 254 (2022) 113856.

[12] A.A. Taflanidis, J.L. Beck, Life-cycle cost optimal design of passive dissipative devices, Structural Safety. 31 (2009) 508–522. doi:10.1016/j.strusafe.2009.06.010.

[13] I. Gidaris, A.A. Taflanidis, Performance Assessment and Optimization of Fluid Viscous Dampers Through Life-Cycle Cost Criteria and Comparison to Alternative Design Approaches, Bulletin of Earthquake Engineering. 13 (2015) 1003–1028.

[14] H. Shin, M.P. Singh, Minimum life-cycle cost-based optimal design of yielding metallic devices for seismic loads, Engineering Structures. 144 (2017) 174–184. doi:10.1016/j.engstruct.2017.04.054.

[15] R. Ruiz, A.A. Taflanidis, D. Lopez-Garcia, C.R. Vetter, Life-Cycle Based Design of Mass Dampers for The Chilean Region and Its Application for The Evaluation of the Effectiveness of Tuned Liquid Dampers with Floating Roof, Bulletin of Earthquake Engineering. 14 (2016) 943–970.

[16] H. Shin, M.P. Singh, Minimum failure cost-based energy dissipation system designs for buildings in three seismic regions--Part II: Application to viscous dampers, Engineering Structures. 74 (2014) 275–282. doi:10.1016/j.engstruct.2014.05.012.

[17] Y.K. Wen, Y.J. Kang, Minimum Building Life-Cycle Cost Design Criteria. II: Applications, Journal of Structural Engineering. 127 (2001) 338–346. doi:10.1061/(ASCE)0733-9445(2001)127:3(338).

[18] M. Khalilian, H. Shakib, M.C. Basim, On the optimal performance-based seismic design objective for steel moment resisting frames based on life cycle cost, Journal of Building Engineering. 44 (2021) 103091. doi:10.1016/j.jobe.2021.103091.

[19] H. Varaee, A. Shishegaran, M.R. Ghasemi, The life-cycle cost analysis based on probabilistic optimization using a novel algorithm, Journal of Building Engineering. 43 (2021) 103032. doi:10.1016/j.jobe.2021.103032.

[20] M. Cheng, D.M. Frangopol, Life-cycle optimization of structural systems based on cumulative prospect theory: Effects of the reference point and risk attitudes, Reliability Engineering & System Safety. 218 (2022) 108100. doi:10.1016/j.ress.2021.108100.

[21] M.A. Santos-Santiago, S.E. Ruiz, L. Cruz-Reyes, Optimal design of buildings under wind and earthquake, considering cumulative damage, Journal of Building Engineering. 56 (2022) 104760. doi:10.1016/j.jobe.2022.104760.

[22] L.M. Moreschi, M.P. Singh, Design of yielding metallic and friction dampers for optimal seismic performance, Earthquake Engineering & Structural Dynamics. 32 (2003) 1291–1311.

[23] Z. Li, G. Shu, Z. Huang, Proper configuration of metallic energy dissipation system in shear-type building structures subject to seismic excitation, Journal of Constructional Steel Research. 154 (2019) 177–189.

[24] C.A. Martinez, O. Curadelli, M.E. Compagnoni, Optimal placement of nonlinear hysteretic dampers on planar structures under seismic excitation, Engineering Structures. 65 (2014) 89–98.

[25] E. Matta, Lifecycle cost optimization of tuned mass dampers for the seismic improvement of inelastic structures, Earthquake Engineering & Structural Dynamics. 47 (2017) 714–737. doi:10.1002/eqe.2987.

[26] ATC-13, Earthquake Damage Evaluation Data for California, Applied Technology Council, Redwood City, CA, 1985.

[27] FEMA-NIBS, Earthquake Loss Estimation Methodology-HAZUS Technical Manual, Federal Emergency Management Agency and National Institute of Building Sciences, Washington, DC, 2003.

[28] N.A. Kolour, M.C. Basim, M. Chenaghlou, Multi-objective optimum design of nonlinear viscous dampers in steel structures based on life cycle cost, in: Structures,

2021: pp. 3776–3788.

[29] M. Mousazadeh, F. Pourreza, M.C. Basim, M.R. Chenaghlou, An efficient approach for LCC-based optimum design of lead-rubber base isolation system via FFD and analysis of variance (ANOVA), Bulletin of Earthquake Engineering. 18 (2020) 1805–1827. doi:10.1007/s10518-019-00754-6.

[30] S. Kleingesinds, O. Lavan, I. Venanzi, Life-cycle cost-based optimization of MTMDs for tall buildings under multiple hazards, Structure and Infrastructure Engineering. 17 (2021) 921–940.

[31] O. Idels, O. Lavan, Performance-based seismic retrofitting of frame structures using negative stiffness devices and fluid viscous dampers via optimization, Earthquake Engineering \& Structural Dynamics. 50 (2021) 3116–3137.

[32] H.E. Estekanchi, A. Vafai, M. Sadeghazar, Endurance time method for seismic analysis and design of structures, Scientia Iranica. 11 (2004) 361–370.

[33] FEMA P-58-1, Seismic Performance Assessment of Buildings, Volume 1 - Methodology, Federal Emergency Management Agency, Federal Emergency Management Agency: Washington, DC, 2018.

[34] A. Rahgozar, H.E. Estekanchi, S.A. Mirfarhadi, On optimal triple friction pendulum base-isolation design for steel moment-frame buildings employing value-based seismic design methodology, Journal of Building Engineering. 63 (2023) 105494. doi:10.1016/j.jobe.2022.105494.

[35] ANSI/AISC 360, Specification for Structural Steel Buildings, American Institute for Steel Construction, Chicago, IL, 2022.

[36] R.K. McGuire, Probabilistic Seismic Hazard Analysis: Early History, Earthquake Engineering & Structural Dynamics. 37 (2008) 329–338. doi:10.1002/eqe.765.

[37] M. Mashayekhi, H.E. Estekanchi, H. Vafai, S.A. Mirfarhadi, Development of hysteretic energy compatible endurance time excitations and its application, Engineering Structures. 177 (2018) 753–769. doi:10.1016/j.engstruct.2018.09.089.

[38] J. Bai, S. Jin, J. Zhao, B. Sun, Seismic performance evaluation of soil-foundation-reinforced concrete frame systems by endurance time method, Soil Dynamics and Earthquake Engineering. 118 (2019) 47–51. doi:10.1016/j.soildyn.2018.12.011.

[39] A. Shirkhani, B.F. Azar, M.C. Basim, Seismic loss assessment of steel structures equipped with rotational friction dampers subjected to intensifying dynamic excitations, Engineering Structures. 238 (2021) 112233.

[40] H.A. Amiri, E.P. Najafabadi, H.E. Estekanchi, T. Ozbakkaloglu, Performance-based seismic design and assessment of low-rise steel special moment resisting frames with block slit dampers using endurance time method, Engineering Structures. 224 (2020) 110955.

[41] M. Tavakolinia, M. Ch. Basim, Performance-based optimum tuning of tuned mass dampers on steel moment frames for seismic applications using the endurance time method, Earthquake Engineering \& Structural Dynamics. 50 (2021) 3646–3669.

[42] A.S. Movahhed, A. Shirkhani, S. Zardari, M. Mashayekhi, E.N. Farsangi, A. Majdi, Modified endurance time method for seismic performance assessment of base-isolated structures, Journal of Building Engineering. 67 (2023) 105955.

[43] J. Huang, P. Tan, Y. Zhang, F. Zhou, Endurance time analysis of seismic performances

of long-span continuous rigid-frame bridges with corrugated steel webs, in: Structures, 2022: pp. 990–1001.

[44] Q. Xu, T. Zhang, J. Chen, J. Li, S. Xu, A new endurance time analysis method for damage evaluation of high arch dams under the oblique incidence of mainshock-aftershock seismic sequences by wavelet decomposition, Soil Dynamics and Earthquake Engineering. 161 (2022) 107406.

[45] C. Xu, H. Luo, Y. Wu, Z. Wang, Effects of modelling uncertainty on the seismic fragility of frame piers in double-deck viaducts, Structure and Infrastructure Engineering. (2023) 1–12.

[46] H.E. Estekanchi, Endurance Time Method Website, (2023). www.sites.google.com/site/etmethod (accessed April 12, 2023).

[47] The Gordian Group, RSMeans Data, 2023. https://www.rsmeans.com.

[48] H.S. Banzhaf, The value of statistical life: A meta-analysis of meta-analyses, Journal of Benefit-Cost Analysis. 13 (2022) 182–197.

[49] DOT, Treatment of the Value of Preventing Fatalities and Injuries in Preparing Economic Analyses, U.S. Department of Transportation, 2021.

[50] S.A. Mirfarhadi, H.E. Estekanchi, M. Sarcheshmehpour, On optimal proportions of structural member cross-sections to achieve best seismic performance using value based seismic design approach, Engineering Structures. 231 (2021) 111751. doi:10.1016/j.engstruct.2020.111751.

[51] J. Kennedy, R. Eberhart, Particle swarm optimization, in: Proc. ICNN'95-International Conf. Neural Networks, 1995: pp. 1942–1948.

[52] NIST GCR 10-917-8, Evaluation of the FEMA P-695 Methodology for Quantification of Building Seismic Performance Factors, NEHRP consultants Joint Venture, 2010.

[53] ASCE/SEI 7-22, Minimum Design Loads and Associated Criteria for Buildings and Other Structures, American Society of Civil Engineers, Reston, VA, 2022.

[54] C. Xia, R.D. Hanson, Influence of ADAS element parameters on building seismic response, Journal of Structural Engineering. 118 (1992) 1903–1918.

[55] OpenSees, Open System for Earthquake Engineering Simulation version 3.3.0 [Software], (2022). https://opensees.berkeley.edu/.

[56] L.F. Ibarra, R.A. Medina, H. Krawinkler, Hysteretic Models That Incorporate Strength and Stiffness Deterioration, Earthquake Engineering & Structural Dynamics. 34 (2005) 1489–1511. doi:10.1002/eqe.495.

[57] D.G. Lignos, H. Krawinkler, Deterioration Modeling of Steel Components in Support of Collapse Prediction of Steel Moment Frames under Earthquake Loading, Journal of Structural Engineering. 137 (2011) 1291–1302. doi:10.1061/(ASCE)ST.1943-541X.0000376.

[58] D.G. Lignos, A.R. Hartloper, A. Elkady, G.G. Deierlein, R. Hamburger, Proposed updates to the ASCE 41 nonlinear modeling parameters for wide-flange steel columns in support of performance-based seismic engineering, Journal of Structural Engineering. 145 (2019) 4019083.

[59] A. Gupta, H. Krawinkler, Seismic demands for the performance evaluation of steel moment resisting frame structures, Stanford University, 1998.

[60] G. Brando, F. D'Agostino, G. De Matteis, Seismic performance of MR frames protected by viscous or hysteretic dampers, The Structural Design of Tall and Special Buildings. 24 (2015) 653–671.

[61] F. Zareian, R.A. Medina, A practical method for proper modeling of structural damping in inelastic plane structural systems, Computers & Structures. 88 (2010) 45–53. doi:10.1016/j.compstruc.2009.08.001.

[62] G.J. Hoffman, A.E. Thal Jr, T.S. Webb, J.D. Weir, Estimating performance time for construction projects, Journal of Management in Engineering. 23 (2007) 193–199.

[63] FEMA P-58-3, Seismic Performance Assessment of Buildings, Volume 3 - Supporting Electronic Materials, Federal Emergency Management Agency, Washington, DC, 2018.

[64] USGS, United States Geological Survey, United States Geological Survey. (2023). https://www.usgs.gov (accessed April 12, 2023).

[65] M.R. Mashayekhi, S.A. Mirfarhadi, H.E. Estekanchi, H. Vafai, Predicting probabilistic distribution functions of response parameters using the endurance time method, The Structural Design of Tall and Special Buildings. 28 (2019) e1553. doi:10.1002/tal.1553.

Conflict of Interest (Please upload in Word format)

Declaration of interests

☒ The authors declare that they have no known competing financial interests or personal relationships that could have appeared to influence the work reported in this paper.

☐The authors declare the following financial interests/personal relationships which may be considered as potential competing interests: